Thermodynamics of exotic black holes in Lovelock gravity

Brayden Hull[*] and Robert B. Mann[†]

Department of Physics and Astronomy, University of Waterloo, Waterloo, Ontario, Canada, N2L 3G1, Perimeter Institute for Theoretical Physics, 31 Caroline St. N., Waterloo, Ontario, N2L 2Y5, Canada, and Waterloo Center for Astrophysics, University of Waterloo, Waterloo Ontario, Canada, N2L 3G1

(Received 10 March 2021; accepted 11 August 2021; published 4 October 2021)

We examine the thermodynamics of a new class of asymptotically anti–de Sitter (AdS) black holes with nonconstant curvature event horizons in Gauss-Bonnet Lovelock gravity, with the cosmological constant acting as thermodynamic pressure. We find that nontrivial curvature on the horizon can significantly affect their thermodynamic behavior. We observe novel triple points in six dimensions between large and small uncharged black holes and thermal AdS. For charged black holes we find a continuous set of triple points whose range depends on the parameters in the horizon geometry. We also find new generalizations of massless and negative mass solutions previously observed in Einstein gravity.

DOI: 10.1103/PhysRevD.104.084032

I. INTRODUCTION

Einstein's general theory of relativity is an extremely elegant and successful theory of gravitation, passing all of its experimental tests since its inception over 100 years ago [1]. Yet its reconciliation with quantum theory remains elusive. While there is yet to be a proper full description of quantum gravity, a key piece of the puzzle is provided by black holes. Originally thought to be nature's ultimate repositories of matter and energy, their behavior drastically changes once quantum physics is taken into account [2], leading to the well-known prediction that a black hole radiates like a thermal blackbody whose temperature is proportional to its surface gravity and whose entropy is proportional to its horizon area. In anti–de Sitter spacetime, they can undergo phase transitions [3] and in fact exhibit a very broad range of chemical thermodynamics [4].

Another general expectation that emerges from quantum gravity is the presence of higher curvature terms that correct the Einstein-Hilbert action [5,6]. The most commonly discussed is Lovelock gravity [7], which is regarded as a physically sensible generalization of Einstein gravity to higher dimensions since its field equations are second order in all metric components. These theories have the general feature that the entropy of a black hole is no longer proportional to the horizon area, and so are of particular interest in black hole thermodynamics since they provide a window into how quantum gravitational effects could modify the radiative behavior of black holes [8].

So far work on black hole thermodynamics in Lovelock gravity has been limited to black hole solutions that have a constant curvature manifold as its transverse space. However, this limitation is not necessary: recently, a more general class of black hole solutions were found for Lovelock gravity in which the transverse space is a more general manifold [9]. Such solutions take the form of a warped product of a two-dimensional space and an arbitrary transverse base manifold [10–15]. There is a generalization of the Birkhoff theorem that implies this base manifold must be static. Furthermore, the field equations impose the conditions that all the nontrivial intrinsic Lovelock tensors of the base manifold are constants that can be chosen arbitrarily. We shall refer to such objects as "exotic Lovelock black holes," or ELBHs.

We investigate here the thermodynamic properties of ELBHs in Einstein Maxwell Gauss-Bonnet gravity, the simplest Lovelock gravity theory. ELBHs in this case depend on two parameters, and in the limit that these parameters are chosen so that when the base manifold has constant curvature, we recover thermodynamic phenomena for both neutral and charged black holes previously observed in Gauss-Bonnet gravity [8]. We find that ELBHs exhibit new effects as they increasingly depart from this special case. For example, we observe a novel triple point between thermal radiation and large and small ELBHs in six dimensions. In the $d = 6$ charged case we find that the particular features of the large/intermediate/small triple point depends on the horizon geometry.

We also find an interesting set of massless and negative mass black hole solutions that generalize those found previously in Einstein gravity [16–18]. These have a more interesting structure insofar as two horizons are possible under some circumstances, and their singularity structure is more complicated than the corresponding situation in Einstein gravity.

[*]b2hull@uwaterloo.ca
[†]rbmann@uwaterloo.ca

We first begin with a review of Lovelock gravity, discussing black hole solutions whose transverse spaces are of constant and nonconstant curvature and make a simple distinction between the two, how to transition between each and provide a calculation of the Kretschmann scalar for an arbitrary metric. We follow that with a discussion of Lovelock black hole thermodynamics. In Sec. III, we examine Gauss-bonnet gravity, with first a discussion of vacumm solutions and then five- and six-dimensional black holes (uncharged then charged). In Sec. V, we give a summary of our results and future outlook.

II. EXOTIC LOVELOCK BLACK HOLES

The Lagrangian for a Lovelock theory [7] in d dimensions is

$$\mathcal{L} = \frac{1}{16\pi G_N}\sum_{k=0}^{K}\hat{\alpha}_k\mathcal{L}^{(k)}, \tag{2.1}$$

where $\hat{\alpha}_k$ are the Lovelock coupling constants and $\mathcal{L}^{(k)}$ are the Euler densities,

$$\mathcal{L}^{(k)} = \frac{1}{2^k}\delta^{a_1b_1\ldots a_kb_k}_{c_1d_1\ldots c_kd_k}R^{c_1d_1}_{a_1b_1}\ldots R^{c_kd_k}_{a_kb_k}. \tag{2.2}$$

with the contraction occurring over the antisymmetric generalized Kronecker delta. The dimension of the Euler densities is $2k$, with $\mathcal{L}^{(0)}$ being the cosmological constant, $\mathcal{L}^{(1)}$ the Ricci scalar, and $\mathcal{L}^{(2)}$ the Gauss-Bonnett term. Note that we must have $d > 2K$ in order to have nontrivial field equations.

With the lagragnian (2.1) we can write our action for Lovelock theory as

$$S = \int d^dx\sqrt{-g}\left(\frac{1}{16\pi G_N}\sum_{k=0}^{K}\hat{\alpha}_k\mathcal{L}^{(k)} + \mathcal{L}_{\text{matter}}\right). \tag{2.3}$$

Variation of the action with respect to the metric yields the field equations

$$\sum_{k}^{K}\hat{\alpha}_k\mathcal{G}^{(k)}_{ab} = 8\pi G_N T_{ab}, \tag{2.4}$$

where T_{ab} is the stress-energy tensor and $\mathcal{G}^{(k)}_{ab}$ are the Lovelock tensors

$$\mathcal{G}^{(k)}_{ab} = -\frac{1}{2^{(k+1)}}g_{za}\delta^{zc_1d_1\ldots c_kd_k}_{be_1f_1\ldots e_kf_k}R^{e_1f_1}_{c_1d_1}\ldots R^{e_kf_k}_{c_kd_k}. \tag{2.5}$$

We will be examining charged black holes, which means we will use the following Lagrangian $\mathcal{L}_{\text{matter}} = -4\pi G_N F_{ab}F^{ab}$, which will give us our finalized field equations,

$$\sum_{k=0}^{K}\hat{\alpha}_{(k)}\mathcal{G}^{(k)}_{ab} = 8\pi G_N\left(F_{ac}F^c_b - \frac{1}{4}g_{ab}F_{cd}F^{cd}\right). \tag{2.6}$$

We shall discuss the black hole solutions to these equations in the next section.

A. Black hole solutions

We will be focusing on charged anti–de Sitter (AdS) black hole solutions in this paper, using the ansatz

$$\begin{aligned} ds^2 &= \mathsf{g}_{ij}dy^idy^j + \gamma_{\alpha\beta}dx^\alpha dx^\beta \\ &= -f(r)dt^2 + \frac{dr^2}{f(r)} + r^2d\Sigma^2_{d-2} \\ F &= \frac{Q}{r^{d-2}}dt\wedge dr, \end{aligned} \tag{2.7}$$

for the metric and gauge field strength, that we require to be solutions to (2.6). The coordinates $y^i = (t, r)$, with $\mathsf{g}_{ij} = \text{diag}(-f(r), 1/f(r))$. The importance of this metric lies in the nature of the base manifold described by $d\Sigma^2_{d-2}$.

The most common approach is to take $d\Sigma^2_{d-2}$ to be a $(d-2)$-dimensional compact space of constant curvature given by $(d-2)(d-3)\kappa$, with $\kappa = -1, 0, +1$ corresponding to hyperbolic, flat, or spherical curvature respectively. This yields the polynomial equation [19–23],

$$\begin{aligned} \sum_{k=0}^{K}\alpha_k\left(\frac{\kappa - f(r)}{r^2}\right)^k &= \frac{16\pi GM}{(d-2)\Sigma^{(\kappa)}_{d-2}r^{d-1}} \\ &\quad - \frac{8\pi G_N Q^2}{(d-2)(d-3)}\frac{1}{r^{2d-4}}, \end{aligned} \tag{2.8}$$

from (2.6). Here M is the mass of the black hole, $\Sigma^{(\kappa)}_{d-2}$ is the volume of the compact space whose metric is $d\Sigma^2_{d-2}$. Q is the black hole charge given by

$$Q = \frac{1}{2\Sigma^{(\kappa)}_{d-2}}\int *F. \tag{2.9}$$

The α_k terms are rescaled Lovelock coupling constants,

$$\begin{aligned} \alpha_0 &= \frac{\hat{\alpha}_{(0)}}{(d-1)(d-2)} = \alpha_1 = \hat{\alpha}_{(1)}, \\ \alpha_k &= \hat{\alpha}_{(k)}\prod_{n=3}^{2k}(d-n) \quad \text{for } k \geq 2, \end{aligned} \tag{2.10}$$

where the cosmological constant $\Lambda = -\hat{\alpha}_{(0)}/2$. In what follows we will set $\alpha_1 = 1$ to retrieve general relativity in the low energy limit.

However it is possible to assume that $d\Sigma^2_{d-2}$ is the metric of a more general $(d-2)$-dimensional base manifold that does not have to be of constant curvature. In this case the field equations (2.6) become

$$\mathcal{G}^i_j \equiv -\frac{(d-2)(d-1)\delta^i_j}{2(d-1)!r^{d-2}}\sum_{n=0}^{\bar{k}}\{(d-2n-2)!\hat{\mathcal{L}}^{(n)}\}\left\{\frac{d}{dr}\left(r^{d-2n-1}A_n\left(\frac{-f(r)}{r^2}\right)\right)\right\} = 8\pi G_N T^i_j \tag{2.11}$$

$$\mathcal{G}^\alpha_\beta \equiv \frac{(d-1)(d-2)}{(d-1)!r^{d-3}}\sum_{n=0}^{\bar{k}}\{(d-2n-3)!\hat{\mathcal{G}}^{(n)\alpha}_\beta\}\left\{\frac{d^2}{dr^2}\left(r^{d-2n-1}A_n\left(\frac{-f(r)}{r^2}\right)\right)\right\} = 8\pi G_N T^\alpha_\beta, \tag{2.12}$$

with the polynomial,

$$A_n\left(\frac{-f(r)}{r^2}\right) \equiv \sum_{k=n}^{K}\alpha_k\binom{k}{n}\left(\frac{-f(r)}{r^2}\right)^{k-n}, \tag{2.13}$$

which satisfies the recurrence relation,

$$A'_n\left(\frac{-f(r)}{r^2}\right) = (n+1)A_{n+1}\left(\frac{-f(r)}{r^2}\right). \tag{2.14}$$

The quantities $\hat{\mathcal{L}}^{(n)}$ and $\hat{\mathcal{G}}^{(n)\alpha}_\beta$ are respectively the Euler characteristic and Lovelock tensors of the base manifold,

$$\hat{\mathcal{L}}^{(n)} = \frac{(d-2)!b_n}{(d-2n-2)!}$$
$$\hat{\mathcal{G}}^{(n)\alpha}_\beta = -\frac{(d-3)!b_n}{2(d-2n-3)!}\delta^\alpha_\beta, \tag{2.15}$$

reducing the field equations to

$$\mathcal{G}^i_j \equiv \frac{-(d-2)\delta^i_j}{2r^{d-2}}\frac{d}{dr}\sum_{n=0}^{K}\left\{b_n\left(r^{d-2n-1}A_n\left(\frac{-f(r)}{r^2}\right)\right)\right\} = 8\pi G_N T^i_j \tag{2.16}$$

$$\mathcal{G}^\alpha_\beta \equiv \frac{-\delta^\alpha_\beta}{2r^{d-3}}\frac{d^2}{dr^2}\sum_{n=0}^{K}\left\{b_n\left(r^{d-2n-1}A_n\left(\frac{-f(r)}{r^2}\right)\right)\right\} = 8\pi G_N T^\alpha_\beta. \tag{2.17}$$

In this case the polynomial equation in $f(r)$ becomes [24]

$$\sum_{n=0}^{K}\frac{b_n}{r^{2n}}\left(\sum_{k=n}^{K}\alpha_k\binom{k}{n}\left(\frac{-f(r)}{r^2}\right)^{k-n}\right) = \frac{16\pi G_N M}{(d-2)\Sigma_{d-2}r^{d-1}} - \frac{8\pi G_N Q^2}{(d-2)(d-3)}\frac{1}{r^{2d-4}}, \tag{2.18}$$

generalizing (2.8). We shall refer to the solutions that follow from solutions to (2.18) in which $f(r)$ vanishes at least once for some $r > 0$ as *exotic Lovelock black holes*, or ELBHs, where the term b_n is introduced and is referred to as the topological parameter. We can set $b_0 = 1$ without any loss of generality.

Before proceeding to the thermodynamics we mention a few more things with regards to the field equations (2.16) and (2.17). Upon comparing the left-hand sides of Eqs. (2.8) and (2.18), we obtain

$$b_n = \kappa^n, \tag{2.19}$$

for black holes whose base manifolds have constant curvature.

We define the mass, using the Hamiltonian formulation, as the conserved charge corresponding to the time translational Killing vector of a background spacetime to which the black hole solutions approach in the asymptotic region. For black holes with maximally symmetric horizons, this is usually chosen as a constant curvature spacetime that solves the field equations [8,25–28]. In our case, we choose this background solution to have identical geometry of the base manifold as that of the black hole solution under consideration while the corresponding metric function $\bar{f}(r)$ solves the equation,

$$\sum_{n=0}^{K}\frac{b_n}{r^{2n}}\left(\sum_{k=n}^{K}\alpha_k\binom{k}{n}\left(\frac{-\bar{f}(r)}{r^2}\right)^{k-n}\right) = 0. \tag{2.20}$$

One might note an apparent discrepancy in the above equation while considering the dimension $d = 2K+1$, since in this case there are $K-1$ constants b_n characterizing the geometry of the base manifold. In this particular dimensionality, b_K does not carry any geometric information of the base manifold but rather corresponds to the choice of the integration constant specifying the background spacetime. This becomes evident if we rewrite the above equation as

$$\sum_{n=0}^{K-1}\frac{b_n}{r^{2n}}\left(\sum_{k=n}^{K}\alpha_k\binom{k}{n}\left(\frac{-\bar{f}(r)}{r^2}\right)^{k-n}\right) = -\frac{b_K\alpha_K}{r^{2K}}. \tag{2.21}$$

For spherical base manifolds, $b_K = 1$ then corresponds to the natural choice of a constant curvature spacetime as the background. We shall adopt the convention that the sum in (2.18) extends up to K for all d, recognizing that if $d = 2K+1$ the parameter b_K corresponds to a convention for choosing M and contains no geometric information.

In analyzing the structure of our solutions, we will find it useful to employ the Kretschmann scalar, which for the metric (2.7) can be written as

$$R^{abcd}R_{abcd} = \left(\frac{d^2f(r)}{dr^2}\right)^2 + 2\frac{(d-2)}{r^2}\left(\frac{df(r)}{dr}\right)^2 + 2\frac{(d-2)(d-3)f(r)^2}{r^4} - 4\frac{R[\gamma]f(r)}{r^4} + \frac{\mathcal{K}[\gamma]}{r^4}, \tag{2.22}$$

where

$$\mathcal{K}[\gamma] = R^{\alpha\beta\mu\nu}R_{\alpha\beta\mu\nu}[\gamma] \tag{2.23}$$

is the Kretschmann scalar of the base manifold.

B. Lovelock black hole thermodynamics

Lovelock black holes of mass M, entropy S, temperature T, and charge Q obey the extended first law and Smarr relations [29,30]

$$\delta M = T\delta S - \frac{1}{16\pi G_N}\sum_h \hat{\Psi}^{(k)}\delta\hat{\alpha}_{(k)} + \Phi\delta Q \tag{2.24}$$

$$(d-3)M = (d-2)TS + \sum_k 2(k-1)\frac{\hat{\Psi}^{(k)}\hat{\alpha}_{(k)}}{16\pi G_N} + (d-3)\Phi Q, \tag{2.25}$$

where we regard the $\hat{\alpha}_{(k)}$ as thermodynamic parameters. The $\hat{\Psi}^{(k)}$ are their respective conjugate thermodynamic potentials, given by

$$\hat{\Psi}^{(k)} = 4\pi T\mathcal{A}^{(k)} + \mathcal{B}^{(k)} + \Theta^{(k)}, \tag{2.26}$$

with

$$\mathcal{B}^{(k)} = -\frac{16\pi k G_N M(d-1)!}{b(d-2k-1)!}\left(-\frac{1}{\ell^2}\right)^{k-1},$$
$$b = \sum_k \frac{\hat{\alpha}_k k(d-1)!}{(d-2k-1)!}\left(-\frac{1}{\ell^2}\right)^{k-1}$$
$$\Theta^{(k)} = \int_\Sigma \sqrt{-g}\mathcal{L}^{(k)}[s] - \int_{\Sigma_{\mathrm{AdS}}}\sqrt{-g_{\mathrm{AdS}}}\mathcal{L}^{(k)}[s_{\mathrm{AdS}}], \tag{2.27}$$

where $\ell^2 = 1/\alpha^{(0)}$ is the "AdS" radius. The spatial hypersurface Σ, with timelike unit normal n^a and induced metric $s_{ab} = g_{ab} + n_a n_b$, extends from the horizon to infinity.

Black holes in Lovelock gravity no longer obey the area relation $S = \frac{A_H}{4}$ but instead have entropy given by [29]

$$S = \frac{1}{4G_N}\sum_k \hat{\alpha}_k\mathcal{A}^{(k)}, \qquad \mathcal{A}^{(k)} = k\int_{\mathcal{H}}\sqrt{\sigma}\mathcal{L}^{(k-1)}, \tag{2.28}$$

where σ is the determinant of the induced metric on the horizon, and $\mathcal{L}^{(k-1)}$ are the corresponding Euler densities.

We will be treating the (negative) cosmological constant as the thermodynamic pressure,

$$P = -\frac{\Lambda}{8\pi G_N} = \frac{\hat{\alpha}_0}{16\pi G_N}, \qquad V = -\hat{\Psi}^{(0)}, \tag{2.29}$$

with V the conjugate thermodynamic volume of the black hole.

1. ELBH thermodynamics

We wish to solve (2.7) to obtain AdS black hole solutions, solutions for which $f(r)$ grows quadratically with r for large r and has $r = r_+ > 0$ as its largest linear zero. Although we could explicitly solve (2.7) in the $K = 2$ Gauss-Bonnet case, this is not necessary as we can employ the Hamiltonian formalism [20,30,31]. We can find the thermodynamic parameters of the black hole without an explicit solution of $f(r)$ for any value of K.

Setting $f(r_+) = 0$, we find

$$M = \frac{\Sigma_{d-2}(d-2)}{16\pi G_N}\sum_{k=0}^{K}\alpha_k b_k r_+^{d-1-2k} + \frac{\Sigma_{d-2}}{2(d-3)}\frac{Q^2}{r_+^{d-3}}. \tag{2.30}$$

$$T = \frac{f'(r_+)}{4\pi} = \frac{1}{4\pi r_+ D(r_+)}\left[\sum_{k=0}^{K} b_k\alpha_k(d-2k-1)r_+^{-2(k-1)} - \frac{8\pi G_N Q^2}{(d-2)r_+^{2(d-3)}}\right], \tag{2.31}$$

where $D(r_+)$ is

$$D(r_+) = \sum_{k=1}^{K} k\alpha_k b_{k-1} r_+^{-2(k-1)}. \tag{2.32}$$

The entropy is given by

$$S = \frac{\Sigma_{d-2}(d-2)}{4G_N}\sum_{k=0}^{K}\frac{k b_{k-1}\alpha_k r_+^{d-2k}}{d-2k}, \tag{2.33}$$

and through the first law it is easy to identify the conjugate potentials,

$$\Psi^{(k)} = \frac{\Sigma_{d-2}(d-2)}{16\pi G_N} r_+^{d-2k}\left[\frac{b_k}{r_+} - \frac{4b_{k-1}\pi kT}{d-2k}\right]. \tag{2.34}$$

The thermodynamic volume is

$$V = -\hat{\Psi}^{(0)} = \frac{16\pi G_N\Psi^{(0)}}{(d-1)(d-2)} = \frac{\Sigma_{d-2}r_+^{d-1}}{d-1}. \tag{2.35}$$

Using (2.29) and (2.31) we obtain the equation of state,

$$P = \frac{d-2}{16\pi G_N}\sum_{k=1}^{K}\frac{\alpha_k}{r_+^2}r_+^{-2(k-1)}[4\pi k b_{k-1} r_+ T - b_k(d-2k-1)] + \frac{Q^2}{2r_+^{2(d-2)}}, \tag{2.36}$$

where r_+ is a function of the thermodynamic volume from (2.35).

We note the nontrivial dependence of the various thermodynamic parameters on the topological constants b_k. This implies that we might expect new phase behavior for ELBHs as compared to their constant curvature counterparts. To investigate this we shall study the Gibbs free energy [4],

$$G(P,T,Q) = M - TS, \tag{2.37}$$

which characterizes the canonical ensemble. A thermodynamically stable state is given by the global minimum of G for any given choice of the parameters. To observe phase transitions, it is most useful to plot G as a function of T, fixing the other parameters.

This, however, is not sufficient to determine a physically acceptable black hole thermodynamic state. We shall also require that

$$\sum_{k=0}^{K}\frac{k b_{k-1}\alpha_k r_+^{d-2k}}{d-2k} \geq 0, \tag{2.38}$$

so that the entropy is not negative. Likewise, we shall only consider $T \geq 0$ in (2.31). However we shall not require that $M > 0$, since it is known that, for example, topological black holes can have negative masses that are bounded from below [16].

III. ELBHS IN GAUSS-BONNET GRAVITY

We now specialize our considerations to the $K = 2$ Gauss-Bonnet case.

A. Solutions

Setting $K = 2$, in (2.18) we obtain the polynomial equation for $f(r) \equiv f$ in Gauss-Bonnet-Lovelock gravity (where we recall $b_0 = 1$ and $\alpha_1 = 1$),

$$\frac{\alpha_2 f^2}{r^4} + \left(-\frac{1}{r^2} - \frac{2b_1\alpha_2}{r^4}\right)f + \alpha_0 + \frac{b_1}{r^2} + \frac{b_2\alpha_2}{r^4} = \frac{16\pi M}{(d-2)\Sigma_{d-2}r^{d-1}} - \frac{8\pi Q^2}{(d-2)(d-3)r^{2d-4}}, \tag{3.1}$$

whose solutions are

$$f = f_\pm(\mathsf{m},\mathsf{q}) \equiv \frac{r^2 + 2b_1\alpha_2 \pm \sqrt{(b_1^2 - b_2)4\alpha_2^2 + r^4(1-4\alpha_2\alpha_0) + \frac{8\mathsf{m}\alpha_2}{r^{d-5}} - \frac{4\mathsf{q}^2\alpha_2}{r^{2(d-4)}}}}{2\alpha_2}, \tag{3.2}$$

where

$$\mathsf{m} \equiv \frac{8\pi M}{(d-2)\Sigma_{d-2}} \qquad \mathsf{q}^2 \equiv \frac{8\pi Q^2}{(d-2)(d-3)}. \tag{3.3}$$

The solution $f_-(\mathsf{m},\mathsf{q})$ has the limit,

$$\lim_{\alpha_2\to 0} f_-(\mathsf{m},\mathsf{q}) = \alpha_0 r^2 + b_1 - \frac{2\mathsf{m}}{r^{d-3}} + \frac{\mathsf{q}^2}{r^{2(d-3)}}, \tag{3.4}$$

recovering the solution in Einstein gravity for $b_1 = \kappa$.

We also require that $f_\pm(\mathsf{m},\mathsf{q}) \to r^2$ for large r. This implies

$$1 - 4\alpha_2\alpha_0 \geq 0, \tag{3.5}$$

independent of the b_k. Equation (3.5) implies from (2.29) that there is a maximum pressure [8],

$$P \leq P_{\max} = \frac{(d-1)(d-2)}{64\pi\alpha_2}, \tag{3.6}$$

such that if this bound is violated the spacetime is no longer asymptotically AdS.

The horizons are located at

$$r_\pm^2(\mathsf{m},\mathsf{q}) = -\frac{1}{2(\alpha_0 - \frac{2\mathsf{m}}{r_\pm^{d-5}} - \frac{\mathsf{q}^2}{r_\pm^{2(d-4)}})}\left(b_1 \pm \sqrt{b_1^2 - 4b_2\alpha_2\alpha_0 + b_2\alpha_2\left(\frac{8\mathsf{m}}{r_\pm^{d-5}} - \frac{4\mathsf{q}^2}{r_\pm^{2(d-4)}}\right)}\right), \tag{3.7}$$

which implicitly defines $r_\pm$. We note from this that solutions with $\mathsf{m} = \mathsf{q} = 0$

$$f_\pm(0,0) = \frac{r^2 + 2b_1\alpha_2 \pm \sqrt{(b_1^2 - b_2)4\alpha_2^2 + r^4(1 - 4\alpha_2\alpha_0)}}{2\alpha_2} \tag{3.8}$$

have horizons at

$$r_\pm^2(0,0) = \frac{1}{2\alpha_0}\left(-b_1 \pm \sqrt{b_1^2 - 4b_2\alpha_2\alpha_0}\right), \tag{3.9}$$

provided either

$$\text{(a) } b_2 < 0 \quad \text{and} \quad b_1 > 0 \Rightarrow r_+(0,0) \text{ is the only horizon,} \tag{3.10}$$

or, if $b_2 > 0$,

$$\text{(b) } b_1^2 > 4b_2\alpha_2\alpha_0 \quad \text{and} \quad 0 > b_1 > -\sqrt{\frac{b_2}{2(1 - 2\alpha_2\alpha_0)}}$$
$$\Rightarrow r_\pm(0,0) \text{ are both horizons,} \tag{3.11}$$

or

$$\text{(c) } b_1^2 > 4b_2\alpha_2\alpha_0 \quad \text{and} \quad -\sqrt{\frac{b_2}{2(1 - 2\alpha_2\alpha_0)}} > b_1$$
$$\Rightarrow r_+(0,0) \text{ is the only horizon,} \tag{3.12}$$

where the inequalities (3.11) ensure that $r_-(0,0)$ is real and larger than the location of the spacetime singularity.

If any of these conditions do not hold then the solution has a naked singularity.

The solutions (3.8) are generalizations of massless topological black holes in Einstein gravity [16–18], with $\alpha_2 = 0$ and $b_1 = -1$, with appropriate identifications made on the transverse base space [17,32]. Here we have a richer set of possibilities insofar as two horizons are possible, as long as $b_2\alpha_2 > 0$. Negative mass solutions are likewise possible.

An evaluation of the Kretschmann scalar (2.22) for the solution (3.8) yields

$$\begin{aligned} R^{abcd}R_{abcd} = {} & \frac{1}{\alpha_2} + \frac{-48({b_1}^2 - b_2)r^2\alpha_0{\alpha_2}^3 + 12r^2(4r^4{\alpha_0}^2/3 + {b_1}^2 - b_2)\alpha_2^2 - 8\alpha_0\alpha_2 r^6}{\alpha_2((b_1^2 - b_2)4\alpha_2^2 + r^4(1 - 4\alpha_2\alpha_0))^{3/2}} \\ & - 2\frac{(d-2)(-4\alpha_0\alpha_2 r^2 + r^2 + \sqrt{(b_1^2 - b_2)4\alpha_2^2 + r^4(1 - 4\alpha_2\alpha_0)})^2}{\alpha_2^2((b_1^2 - b_2)4\alpha_2^2 + r^4(1 - 4\alpha_2\alpha_0))} \\ & + \frac{(d-2)(d-3)(r^2 + 2b_1\alpha_2 + \sqrt{(b_1^2 - b_2)4\alpha_2^2 + r^4(1 - 4\alpha_2\alpha_0)})^2}{2r^4\alpha_2^2} \\ & - 2\frac{R[\gamma](r^2 + 2b_1\alpha_2 + \sqrt{(b_1^2 - b_2)4\alpha_2^2 + r^4(1 - 4\alpha_2\alpha_0)})}{\alpha_2 r^4} + \frac{K[\gamma]}{r^4}, \end{aligned} \tag{3.13}$$

which clearly has singularities at $r = 0$ and at

$$r_s = \left(\frac{(b_2 - b_1^2)4\alpha_2^2}{1 - 4\alpha_2\alpha_0}\right)^{\frac{1}{4}}. \tag{3.14}$$

Imposing the condition (3.5), it is straightforward to show that the inner horizon $r_-(0,0) > r_s$ provided (3.11) holds; otherwise $r_+(0,0) > r_s$ if either of (3.10) or (3.12) hold. If $b_2 < b_1^2$ the singularity in (3.14) is absent, but the $r = 0$ singularity in general remains. If $b_2 = b_1^2$ the spacetime is of constant curvature and all singularities are absent.

B. Equation of state

The equation of state (2.36) for $K = 2$ is

$$\begin{aligned} P = {} & \frac{(d-2)T}{4r_+} - \frac{(d-2)(d-3)b_1}{16\pi r_+^2} + \frac{(d-2)\alpha_2 b_1 T}{2r_+^3} \\ & - \frac{(d-2)(d-5)\alpha_2 b_2}{16\pi r_+^4} + \frac{Q^2}{2r_+^{2(d-2)}} \end{aligned} \tag{3.15}$$

and becomes

$$\begin{aligned} p = {} & \frac{t}{v} - \frac{(d-2)(d-3)b_1}{4\pi v^2} + \frac{2b_1 t}{v^3} - \frac{(d-2)(d-5)b_2}{4\pi v^4} \\ & + \frac{q^2}{v^2(d-2)}, \end{aligned} \tag{3.16}$$

upon introducing the dimensionless variables (v, t, m, q, p) [8],

$$r_+ = v\alpha_2^{\frac{1}{2}}, \qquad T = \frac{t\alpha_2^{-\frac{1}{2}}}{d-2}, \qquad m = \frac{16\pi M}{(d-2)\Sigma_{d-2}}\alpha_2^{\frac{d-3}{2}},$$
$$Q = \frac{q}{\sqrt{2}}\alpha_2^{\frac{d-3}{2}}, \qquad P = \frac{p}{4\alpha_2}, \tag{3.17}$$

and recalling (3.6) it becomes

$$p \leq p_{\max} = \frac{(d-1)(d-2)}{16\pi}. \tag{3.18}$$

Critical points are obtained by solving

$$\frac{\partial p}{\partial v} = 0, \qquad \frac{\partial^2 p}{\partial v^2} = 0, \tag{3.19}$$

where the first equation determines critical temperature and the latter yields the critical volume. We obtain

$$t_c = \frac{(-4v_c^{8-2d}q^2\pi + b_1(d-3)v_c^2 + 2b_2(d-5))(d-2)}{2\pi(v_c^2 + 6b_1)v_c}, \tag{3.20}$$

and

$$(48v_c^{8-2d}\pi d b_1 + 8v_c^{10-2d}\pi d - 168v_c^{8-2d}\pi b_1 - 20v_c^{10-2d}\pi)q^2 + (-db_1 + 3b_1)v_c^4 + (6db_1^2 - 6b_2 d - 18b_1^2 + 30b_2)v_c^2 - 12db_1b_2 + 60b_1b_2 = 0. \tag{3.21}$$

The Gibbs free energy can also be written in dimensionless form using (3.17) as

$$g = \frac{1}{\Sigma_{d-2}^{(\kappa)}}\alpha_2^{\frac{3-d}{2}}G, \tag{3.22}$$

yielding

$$g = \frac{(d-2)(\frac{v^{d-2}}{d-2} + \frac{2b_1v^{d-4}}{d-4})(\frac{4\pi pv^2}{d-2} + (d-3)b_1 + \frac{(d-5)b_2}{v^2})}{16\pi v(1+\frac{2b_1}{v^2})} + \frac{(d-2)(\frac{4\pi pv^{d-1}}{(d-1)(d-2)} + b_1v^{d-3} + b_2v^{d-5})}{16\pi} + \frac{q^2((2d-5)(d-4)v^2 + 2b_1(d-2)(2d-7))}{4(d-4)(d-2)(d-3)(v^2+2b_1)v^{d-3}}, \tag{3.23}$$

from (2.37).

The positive entropy condition (2.38) for $K = 2$ is

$$\frac{r_+^{d-2}}{d-2} + \frac{2\alpha_2 b_1 r_+^{d-4}}{d-4} \geq 0 \Rightarrow \frac{v^{d-2}}{d-2} + \frac{2b_1v^{d-4}}{d-4} \geq 0, \tag{3.24}$$

which is always satisfied for $b_1 > 0$. For $b_1 < 0$,

$$v \geq \sqrt{2\frac{|b_1|(d-2)}{d-4}}, \tag{3.25}$$

implying that the size of the black hole must be sufficiently large for it to have positive entropy.

Finally, we note that the vacuum horizon equation (3.9) becomes

$$v_\pm^2(0,0) = \frac{(d-1)(d-2)}{8\pi p}\left(-b_1 \pm \sqrt{b_1^2 - \frac{16\pi p b_2}{(d-1)(d-2)}}\right), \tag{3.26}$$

using the dimensionless variables (3.17).

C. Five dimensions

In light of our discussion in Sec. II A, in five dimensions we must obey certain conditions in order to have compatibility with the constant curvature case. The conditions are $b_2 = b_1^2$, where $b_1 = -1,\ 0,\ 1$. We shall consider only $b_1 = \pm 1$ in what follows.

With this, we no longer have the possibility of a singularity outside of the origin in vacuum spacetime [which we can see in (3.14) with the $b_2 = b_1^2$ condition]. Our $f(r)$ solution for the vacuum is given by

$$f_\pm(0,0) = \frac{r^2 + 2b_1\alpha_2 \pm \sqrt{r^4(1-4\alpha_2\alpha_0)}}{2\alpha_2}, \tag{3.27}$$

yielding

$$r_\pm^2(0,0) = \frac{(\pm\sqrt{1-4\alpha_2\alpha_0} - 1)b_1}{2\alpha_0}, \tag{3.28}$$

for the horizons. Note that since $1 > 1 - 4\alpha_0\alpha_2 > 0$, there will be two horizons provided $b_1 < 0$. For $1 - 4\alpha_0\alpha_2 = 0$, there are two coincident horizons,

$$r_+^2 = r_-^2 = \frac{-b_1}{2\alpha_0}, \tag{3.29}$$

which corresponds to be being at maximum AdS pressure, where $b_1 < 0$ or else there will be no horizons. As $\alpha_0 \to 0$, the only horizon is

$$\lim_{\alpha_0 \to 0} r_+^2(0,0) = -b_1\alpha_2 \tag{3.30}$$

for $b_1 < 0$, or else no horizons are present. While the former horizon corresponds to a maximum AdS pressure the later corresponds to zero AdS pressure, which shows that as we turn off the cosmological constant we will still

maintain a vacuum singularity as long as we properly choose our topological term b_1.

For nonzero M and Q we obtain (3.2)

$$f = \frac{r^2 + 2b_1\alpha_2 \pm \sqrt{r^4(1-4\alpha_2\alpha_0) + 8\mathsf{m}\alpha_2 - \frac{4q^2\alpha_2}{r^2}}}{2\alpha_2}, \quad (3.31)$$

from (3.2). For $Q = 0$ there is a bound on the mass,

$$\mathsf{m} \geq -\frac{b_1^2(1-4\alpha_0\alpha_2)}{8\alpha_0}, \quad (3.32)$$

which provides a lower (negative) bound for the mass, below which uncharged black hole solutions do not exist.

1. Uncharged ELBH thermodynamics

The five-dimensional uncharged equation of state is given by

$$p = \frac{t}{v} - \frac{3b_1}{2\pi v^2} + \frac{2tb_1}{v^3}, \quad (3.33)$$

where

$$p_{\max} = \frac{3}{4\pi} \approx 0.2387324146 \quad (3.34)$$

is the maximum dimensionless pressure. The Gibbs free energy is

$$g = -\frac{3(\frac{1}{3}v^3 + 2b_1 v)(\frac{4\pi p v^2}{3} + 2b_1)}{16\pi v(1 + \frac{2b_1}{v^2})} + \frac{3(\frac{1}{3}\pi p v^4 + b_1 v^2 + b_2)}{16\pi}. \quad (3.35)$$

The critical temperature and volume are obtained from (3.20) and (3.21),

$$t_c = \frac{3b_1 v_c}{\pi(v_c^2 + 6b_1)}, \qquad v_c^2 - 6b_1 = 0, \quad (3.36)$$

whose solutions are

$$v_c = \sqrt{6b_1}, \quad t_c = \frac{\sqrt{6b_1}}{4\pi}, \quad p_c = \frac{1}{12\pi} = \frac{p_{\max}}{9}. \quad (3.37)$$

We see that we must have positive values of b_1 in order to have real critical points; this in turn ensures the positive entropy condition holds for all black hole sizes.

With the condition that $b_1^2 = b_2$ we can first begin with the constant curvature case, $b_1 = b_2 = 1$. We see the standard Van der Waals behavior [8] shown in Fig. 1. Seen in the center image there is an intersection between large and small black hole branches, indicating a large/small first order phase transition. However these black holes are unstable since their free energy is greater than that of $g = 0$ which corresponds to AdS radiation. Instead, when the large black hole branch crosses the $g = 0$ axis it will undergo a Hawking/Page transition into thermal AdS radiation [3]. The phase diagram for this first order transition is displayed in the right image of Fig. 1. The apparent sharp corner occurs at the critical point $p = p_c$ for the unstable black hole branch. It is actually smooth but corresponds to a very steep rise in pressure as a function of temperature for $p_c < p < p_{\max}$ from the equation of state, as shown in Fig. 2.

It is interesting to compare the phase behavior of uncharged $d = 5$ Gauss-Bonnet black holes considered previously with the present case. As shown in Fig. 3, the coexistence line between the radiation/large black hole phases is very close to that of the small/large black hole

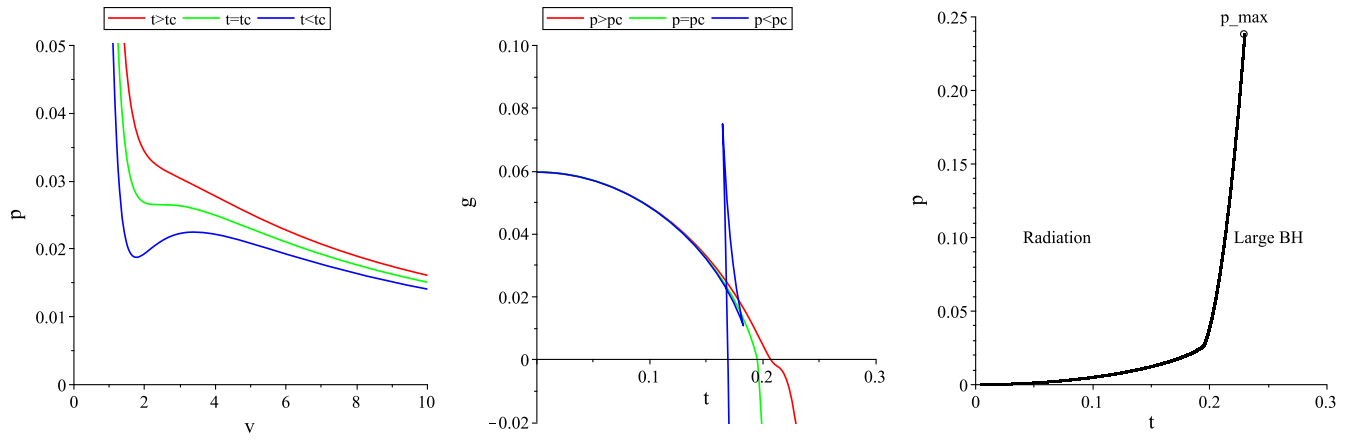

FIG. 1. Phase behavior for $d = 5$, $q = 0$, $b_1 = b_2 = 1$ black holes. *Left:* $p - v$ diagram with constant temperature slices of the *unstable BH* showing the oscillation for $t < t_c$. *Center*: $g - t$ diagram with constant pressure slices around p_c again, of *unstable BHs* showing swallowtail structure with intersection between large and small black holes. *Right:* Phase diagram of the black hole / radiation showing the termination at the maximum pressure.

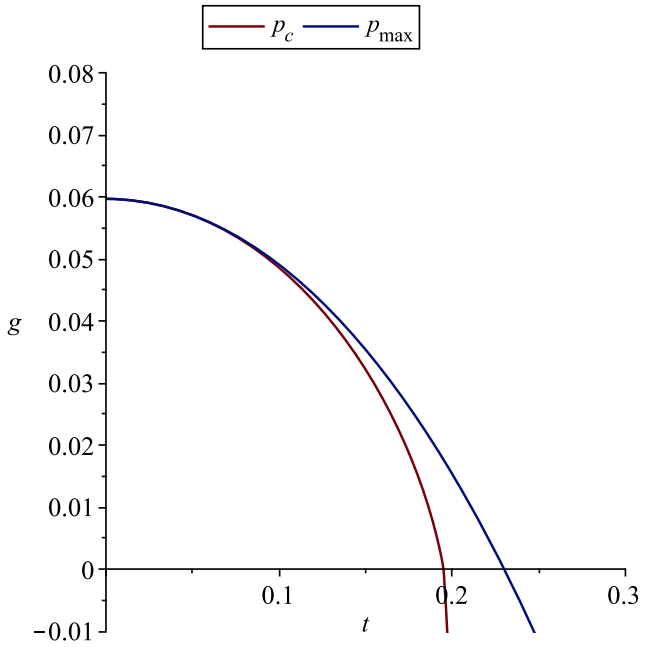

FIG. 2. $g - t$ plots for two constant pressure slices: p_{crit} of the unstable black hole and $p_{\max}$ of the spacetime.

phases. Approaching the diagram from the right, it is clear that as the temperature decreases, the large black hole will undergo a phase transition to radiation before that for a small black hole.

2. Charged ELBH thermodynamics

Including charge, the equation of state and Gibbs free energy are now

$$p = \frac{t}{v} - \frac{3b_1}{2\pi v^2} + \frac{2tb_1}{v^3} + \frac{q^2}{v^6} \tag{3.38}$$

$$g = -\frac{3(\frac{1}{3}v^3 + 2b_1 v)(\frac{4\pi p v^2}{3} + 2b_1)}{16\pi v(1 + \frac{2b_1}{v^2})} + \frac{3(\frac{1}{3}\pi p v^4 + b_1 v^2 + b_2)}{16\pi} + \frac{q^2(5v^2 + 18b_1)}{24(v^2 + 2b_1)v^2}, \tag{3.39}$$

and the critical temperature equation and critical volume relations (3.20) and (3.21) become

$$t_c = \frac{3(b_1 v_c^4 - 2\pi q^2)}{\pi v_c^3(v_c^2 + 6b_1)},$$
$$3v_c^6 b_1 - 18v_c^4 b_1^2 - (30\pi v_c^2 + 108\pi b_1)q^2 = 0. \tag{3.40}$$

Since the latter is a cubic equation in v_c^2, analytic solutions are possible for arbitrary values of b_1 and q. All roots of the cubic will be positive and real only if its coefficients alternate in sign, which is not possible for any values of b_1 or q. Hence there can be at most two admissible solutions for v_c from (3.40).

Plotting in Fig. 4 the critical volume solutions for specific choices of q, we see that negative values of b_1 are permitted as well as positive ones, unlike the uncharged case. For any given charge there is a negative value of b_1 below which there are no longer any real solutions for v_c from (3.40); for $q = 1$ this is approximately $b_1 = -1.5$. As we decrease the charge, the magnitude of the most negative allowed value of b_1 also decreases, as expected since only positive values of b_1 are permitted for $q = 0$.

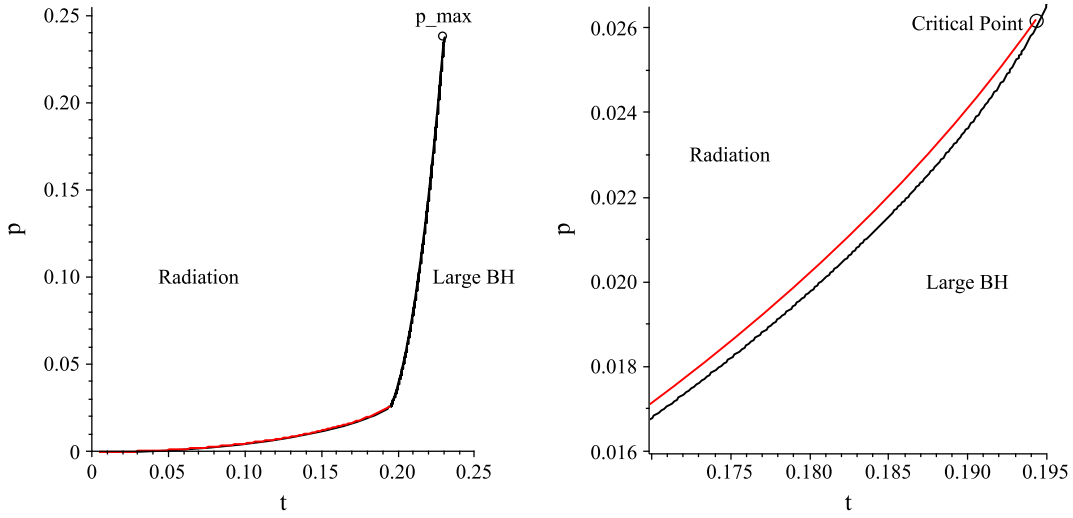

FIG. 3. Left: Phase diagram showing the first-order coexistence line of the unstable large/small transition (red) and the coexistence line of the Hawking-Page transition (black). Right: Close-up version of the left diagram. The unstable small black hole phase is between the red and black lines.

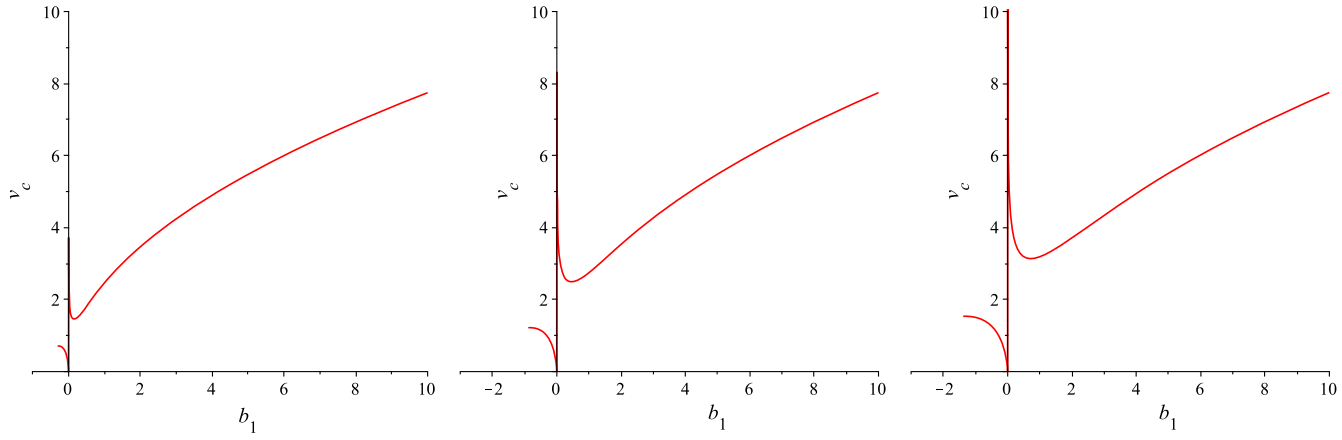

(a) $q = 0.1$ (b) $q = 0.5$ (c) $q = 1$

FIG. 4. Critical volume solutions vs b_1 for varying values of q, the topological parameter b_2 does not play a role in these solutions.

For $b_1 > 0$, there is always a positive root to the cubic, so all positive values of b_1 yield a positive critical volume.

We first begin with $q = 1$, $b_1 = b_2 = 1$, illustrating the results in Fig. 5. In this configuration they exhibit the standard Van der Waals behavior of a large/small black hole phase transition [8]. There is no transition into radiation (thermal AdS) due to conservation of charge. This behavior is qualitatively the same for all possible values of $b_1 > 0$.

We illustrate the situation for $b_1 = -1$ (and $b_2 = 1$) in Fig. 6. In this case there is no Van der Waals type behavior for $p < p_{\max}$ and no interesting phase behavior.

D. Six dimensions

In six dimensions we are free to choose our own values of b_1 and b_2. In this case a vacuum singularity could occur at

$$v = \left(\frac{4(b_2 - b_1^2)}{1 - \frac{4p\pi}{5}}\right)^{\frac{1}{4}}, \tag{3.41}$$

provided $b_2 - b_1^2 > 0$, since $p < p_{\max} = \frac{5}{4\pi} = 0.3978873576$. The vacuum horizon equation (3.9) can be rewritten as

$$v_{\pm}^2(0,0) = \frac{5}{2\pi p}\left(-b_1 \pm \sqrt{b_1^2 - \frac{4\pi p b_2}{5}}\right), \tag{3.42}$$

using the dimensionless variables (3.17).

Now we can re-write the vacuum horizon conditions into dimensionless form as follows:

$$\text{(a) } b_2 < 0 \quad \text{and} \quad b_1 > 0 \Rightarrow v_+(0,0) \text{ is the only horizon,} \tag{3.43}$$

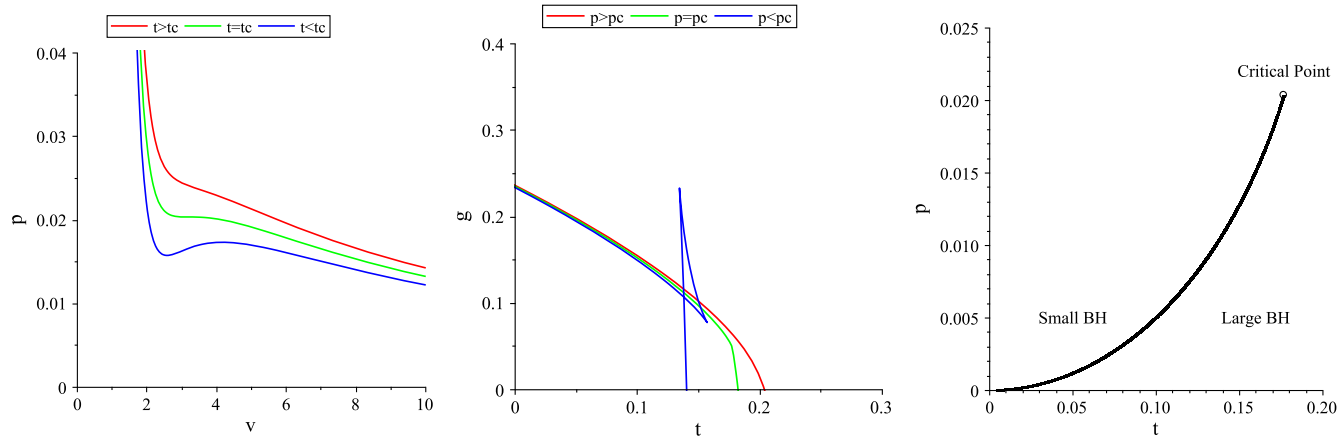

FIG. 5. Phase behavior for $d = 5$, $q = 1$, $b_1 = b_2 = 1$ black holes. *Left:* $p - v$ diagram with constant temperature values mimicking the uncharged case with Van der Waals oscillation. *Bottom:* $g - t$ diagram with constant pressure slices showing large/small branch intersection. *Right:* phase diagram displaying first order transition terminating at the critical point.

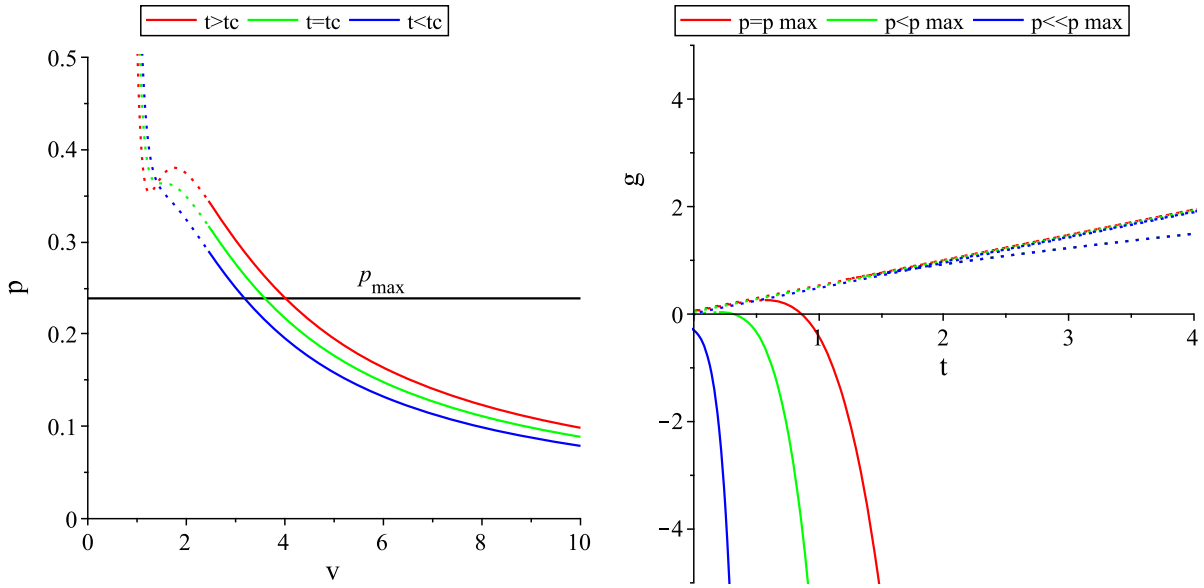

FIG. 6. Phase behavior for $d = 5$, $q = 1$, $b_1 = -1$, $b_2 = 1$ black holes. *Left:* $p - v$ diagram for constant temperature slices. *Right:* $g - t$ diagram for constant pressure slices beginning with maximum pressure and decreasing. Solid lines represent black holes with positive entropy while dotted lines correspond to negative entropy.

or, if $b_2 > 0$,

$$\text{(b) } b_1^2 > \frac{4\pi p b_2}{5} \quad \text{and} \quad 0 > b_1 > -\sqrt{\frac{b_2}{2(1-\frac{2\pi p}{5})}} \Rightarrow v_\pm(0,0) \text{ are both horizons,} \tag{3.44}$$

or

$$\text{(c) } b_1^2 > \frac{4\pi p b_2}{5} \quad \text{and} \quad -\sqrt{\frac{b_2}{2(1-\frac{2\pi p}{5})}} > b_1 \Rightarrow v_+(0,0) \text{ is the only horizon.} \tag{3.45}$$

For nonzero M and Q we have

$$f = \frac{r^2 + 2b_1\alpha_2 \pm \sqrt{r^4(1-4\alpha_2\alpha_0) + \frac{8\mathsf{m}\alpha_2}{r} - \frac{4\mathsf{q}^2\alpha_2}{r^4}}}{2\alpha_2}, \tag{3.46}$$

from (3.2). For $Q = 0$ we obtain

$$\mathsf{m} \geq \mathsf{m}_\pm \equiv -\frac{\sqrt{10}\sqrt{-\alpha_0(3b_1 \pm \sqrt{-20\alpha_0\alpha_2 b_2 + 9b_1^2})}(-3b_1^2 \mp \sqrt{9b_1^2 - 20\alpha_0\alpha_2 b_2} + 20\alpha_0\alpha_2 b_2)}{500\alpha_0^2}, \tag{3.47}$$

as a lower (negative) bound for the mass, below which uncharged black hole solutions do not exist, with m_+ corresponding to $b_1 > 0$ and m_- to $b_1 < 0$. Note that $\mathsf{m}_+ > \mathsf{m}_-$ (solutions with $b_1 < 0$ can have more negative mass) and that $b_2\alpha_2\alpha_0 < 9b_1^2/20$ for such solutions to exist. If $b_2\alpha_2 > 0$ then only $\mathsf{m}_- < 0$.

1. Uncharged ELBHs

The equation of state and Gibbs free energy for $d = 6$ and $q = 0$ are

$$p = \frac{t}{v} - \frac{3b_1}{\pi v^2} + \frac{2tb_1}{v^3} - \frac{b_2}{\pi v^4} \tag{3.48}$$

$$g = -\frac{(\frac{1}{4}v^4 + b_1 v^2)(\pi p v^2 + 3b_1 + \frac{b_2}{v^2})}{4\pi v(1 + \frac{2b_1}{v^2})} + \frac{\frac{1}{5}\pi p v^5 + b_1 v^3 + b_2 v}{4\pi}. \tag{3.49}$$

The critical temperature relation (3.20) is now

$$t_c = \frac{2(3b_1 v_c^2 + 2b_2)}{\pi v_c (v_c^2 + 6b_1)}, \tag{3.50}$$

and the critical volume relation is (3.21) is

$$6v_c^4 b_1 + (-36b_1^2 + 12b_2)v_c^2 + 24b_1 b_2 = 0, \tag{3.51}$$

whose solutions are

$$v_{c\pm}^2 = \frac{(3b_1^2 \pm \sqrt{(9b_1^2 - b_2)(b_1^2 - b_2)} - b_2)}{b_1}. \tag{3.52}$$

If $b_1 > 0$ then we must have $b_2 \leq b_1^2$ in order that v_c be real and positive. If $b_2 > 0$, then both $v_{c\pm}$ are valid critical solutions. Conversely, if $b_1 < 0$ then we must have either $b_2 < 0$ or $b_2 > 9b_1^2$; if the latter holds both $v_{c\pm}$ are valid critical solutions.

To examine the phase behavior of the uncharged solutions, we first set $b_1 = 1$, with the results displayed in Fig. 7. For $b_2 = 1$, corresponding to the standard horizon geometries [8], we get a cusp structure for the $g - t$ diagram and a maximal pressure in the $p - v$ diagram. There is also a minimum, temperature-dependent volume for which $p = 0$. As in the five-dimensional case, the black hole will undergo a Hawking/Page transition from a large black hole into thermal AdS.

Things become more interesting as the value of b_2 changes. As b_2 decreases, we recover standard Van der Waals behavior with a single oscillation in the $p - v$ diagram and the familiar swallowtail structure in the Gibbs free energy diagram.

Unlike the five-dimensional case, this intersection of the swallowtail occurs below the $g = 0$ axis and therefore is a genuine first order large/small first order phase transition between stable black holes—this transition is generally not

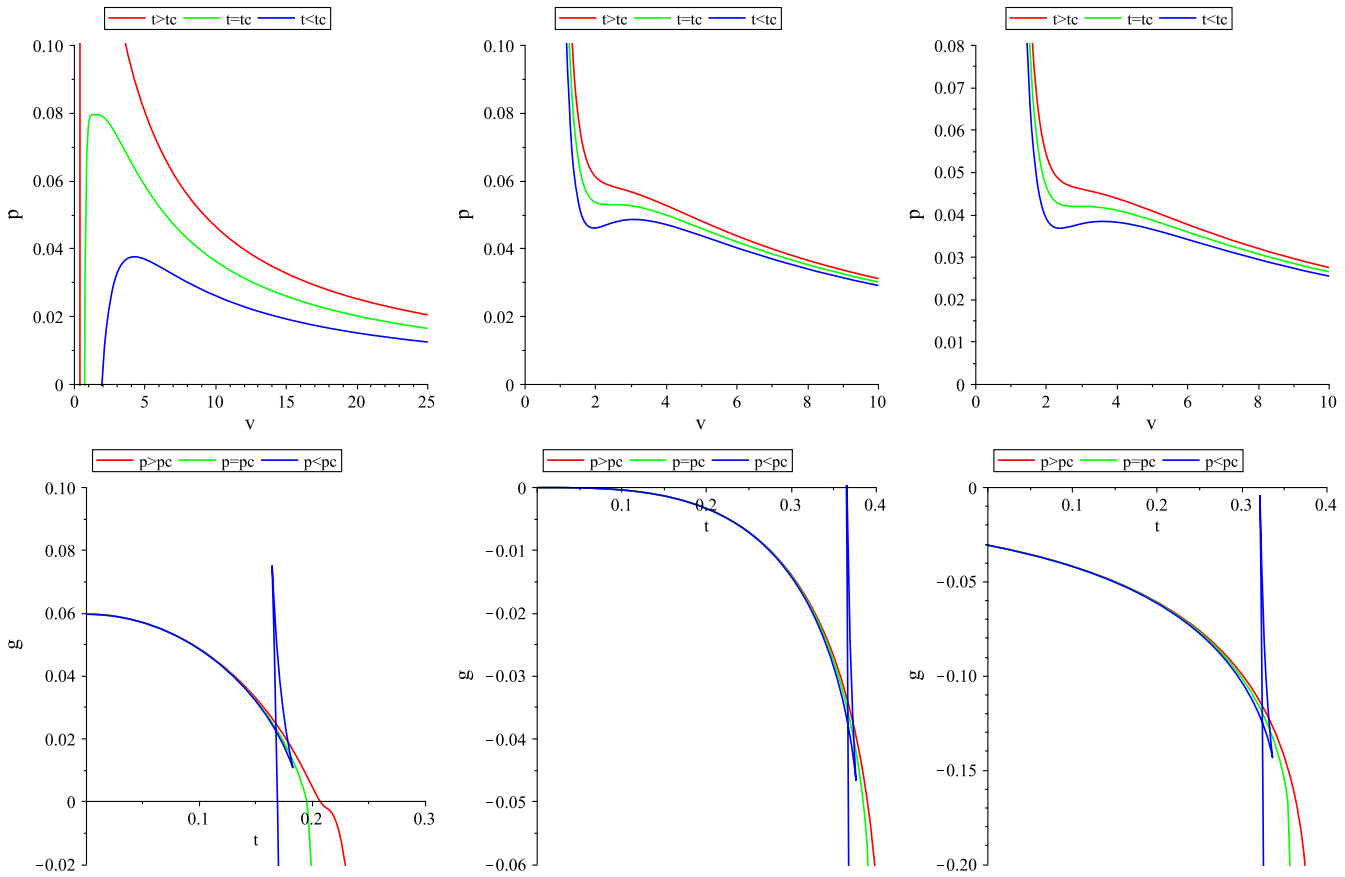

(a) $b_2 = 1$ (b) $b_2 = 0$ (c) $b_2 = -1$

FIG. 7. Phase behavior for $d = 6$, $q = 0$, $b_1 = 1$ black holes. *Top*: Three $p - v$ diagrams for varying values of b_2 at constant temperature slices. *Bottom*: Corresponding $g - t$ plots of constant pressure with b_2 values displayed below. The images on the left display critical temperature/pressure pressures for a nonstable black hole.

observed for uncharged black holes. As b_2 becomes negative, no further qualitative changes in phase behavior are seen.

The phase diagrams are depicted in Fig. 8. Here we can see that when we have $b_2 = 1$ we observe a Hawking/Page transition between a large black hole and thermal AdS, whereas for $b_2 = -1$ we have the standard Van der Waals transition from a large black hole to a small one.

We can notice something between the phase diagram displayed on the right of Fig. 8 and that of the right of Fig. 1. In the five-dimensional case there is a sharp but smooth bend in the diagram, which corresponds to the critical point of the unstable black hole; however in the six-dimensional case the change after this point is not as dramatic. This can be easily explained with reference to the $g - t$ diagram. In the six-dimensional case there is no swallowtail behavior for $b_1 = b_2 = 1$; instead we only observe a cusp. The coexistence curve is correspondingly less sharp, although we still observe a steep slope as $p_{\max}$ is approached. In the $g - t$ diagram, the curves for p_c [the only value that is a solution to (3.19)] and $p_{\max}$ are close together, with only a small difference in temperature between them.

For $1 > b_2 > 0$ swallowtail behavior occurs and the possibility of new phenomenon emerges—that of a new kind of black hole triple point. In Fig. 9 we see (for $b_1 = 1$ and $b_2 = 0.5$) that for $p < p_c$ we can have a large black hole undergoing a first order phase transition into a small black hole that in turn undergoes a transition to thermal AdS as the temperature is lowered further. If we decrease the pressure even further, we arrive at Fig. 10, in which we have the large/small transition occurring on the $g = 0$ axis. This implies a novel triple point where we have the coexistence of large and small black holes with thermal AdS. The phase diagram displaying this novel triple point can be found in Fig. 11. For sufficiently low pressures, there are only two phases, thermal AdS and the large black hole. As the pressure increases, the triple point emerges where the small black hole phase coexists with the other two. At pressures above the novel triple point pressure we observe the three distinct phases as the temperature varies. There is a further critical pressure at which small and large black holes are no longer distinct phases; above this pressure we again have just a single Hawking/Page transtion between thermal AdS and a black hole.

Although within the range of $0 < b_2 < 1$ swallowtail behavior is observed, not all values of b_2 in that range yield a novel-triple point. For $b_1 = 1$ we find only the range $0 < b_2 < \frac{2}{3}$ for which the novel triple point occurs. This can be obtained by solving for the critical volume and temperature, in turn yielding the constraint

$$\frac{(-3b_2+12)\sqrt{b_2^2-10b_2+9}-3b_2^2+31b_2-36}{\pi(\sqrt{b_2^2-10b_2+9}+b_2-3)^2(b_2-9+\sqrt{b_2^2-10b_2+9})}<0, \tag{3.53}$$

that must be satisfied in order to obtain the critical pressure; its solutions are $0 < b_2 < \frac{2}{3}$. If $b_2 = 2/3$, we only have one degenerate critical pressure, at which the novel triple point terminates at the critical point of the black hole, pushing the small branch out and only leaving a large/radiation transition.

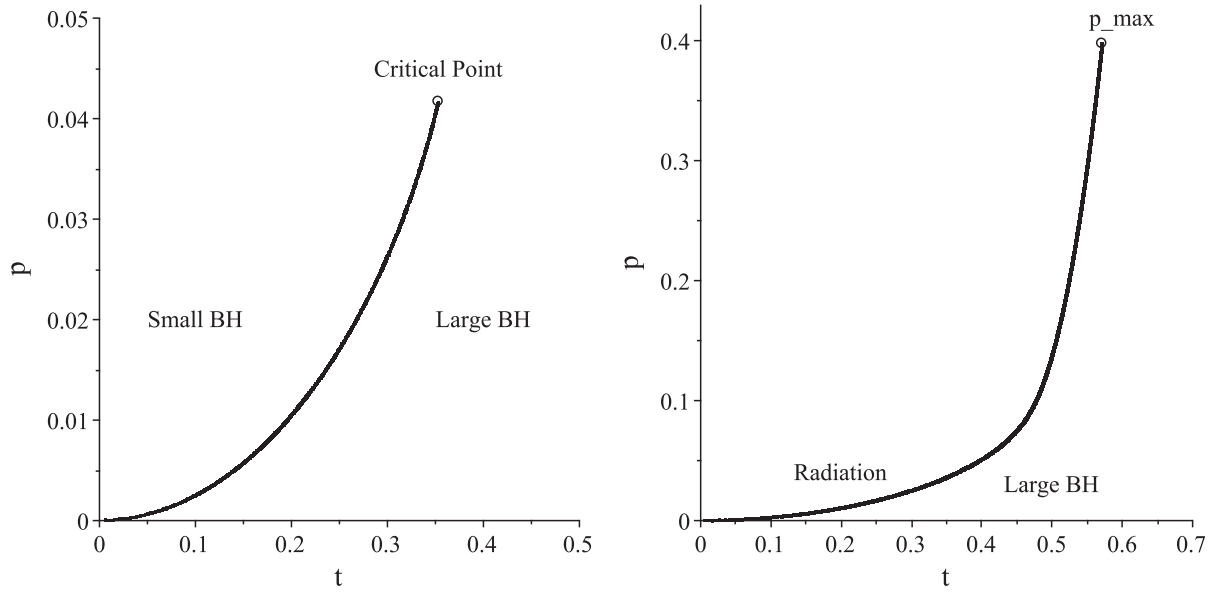

FIG. 8. Coexistence curves for $d = 6$, $q = 0$, $b_1 = 1$ black holes. *Left:* $p - t$ phase diagram for $b_2 = -1$ displaying first order transition between small/large BH, which terminates at the critical point. *Right:* $p - t$ phase diagram for $b_2 = 1$ here we have a transition between Large BH and AdS radiation which terminates at the maximum pressure.

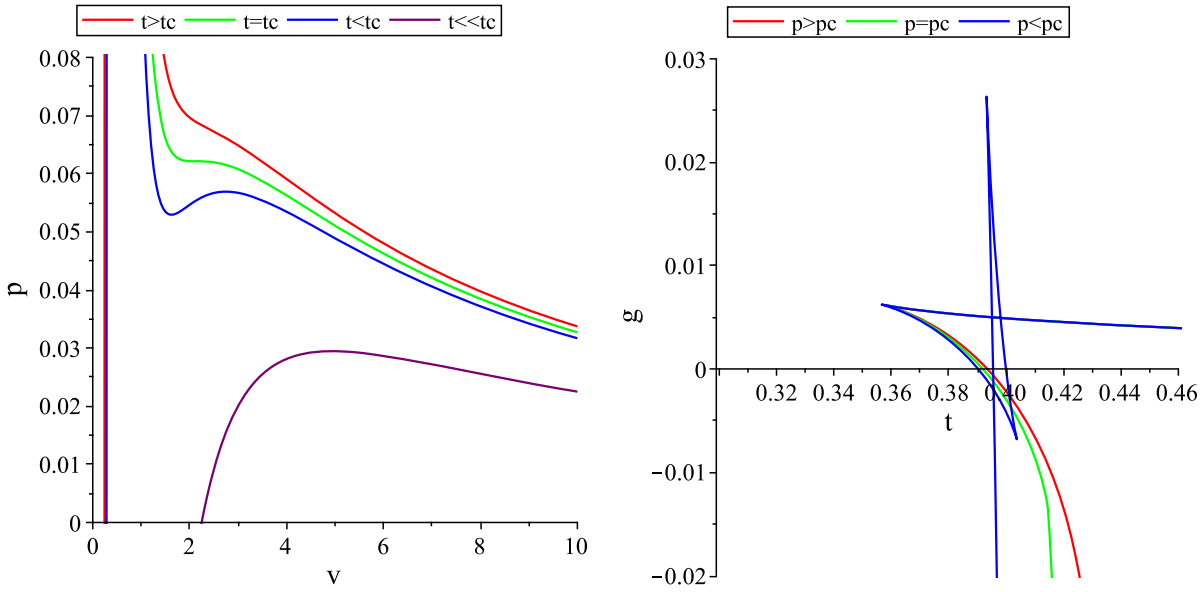

FIG. 9. Phase behavior for $d = 6$, $q = 0$, $b_1 = 1$, $b_2 = 0.5$ black holes. *Left:* $p - v$ diagram for constant temperature slices dislaying Van der Waals oscillations. *Right:* $g - t$ diagram for constant pressure slices.

While the above conditions provide the information needed to know if a triple point is possible, we can also gain information on this from the $g - t$ diagram. In Fig. 12 we see that moving rightward from the cusp on the lower branch, there is a discontinuity in the first derivative of g, indicative of a small/large critical point. If this point is above the $g = 0$ axis no triple point will occur, whereas if it is below then we find the novel triple point. If this point intersects the $g = 0$ axis then the novel triple point merges with the small/large critical point.

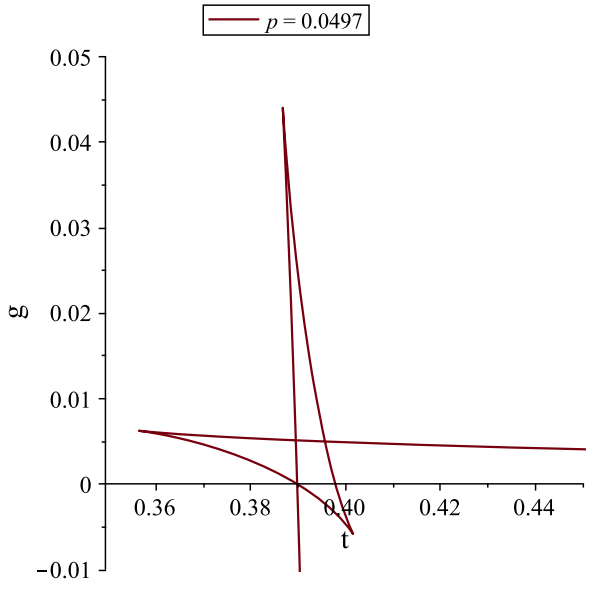

FIG. 10. Novel triple point for $d = 6$, $b_1 = 1$, $b_2 = 0.5$. Gibbs temperature diagram showing the two-branch intersection occurring along the $g = 0$ axis.

Turning to $b_1 < 0$, we must have either $b_2 < 0$ or $b_2 \geq 9b_1^2$ in order to have a real and positive critical volume. However the latter case yields a negative critical temperature, and so critical behavior can take place only for $b_2 < 0$. The only phase behavior we observe in the range $9b_1^2 > b_2 > 0$ is that of a Hawking-Page transition.

We close by noting that throughout this subsection we have chosen $b_2 - b_1 \leq 0$. Hence none of the black holes we

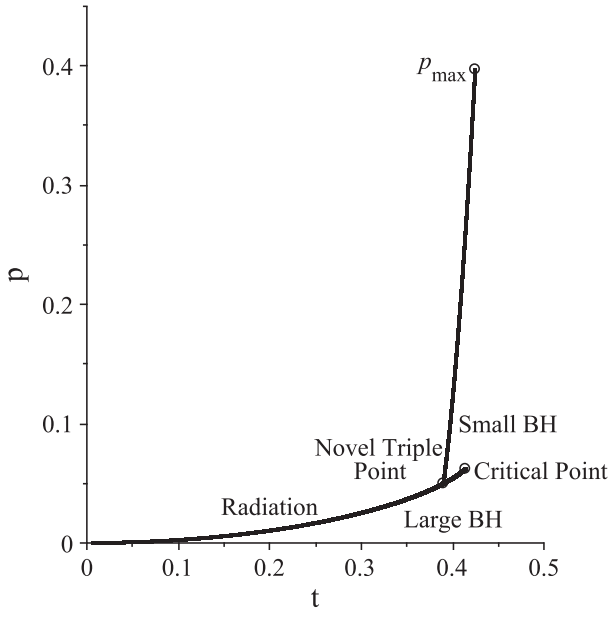

FIG. 11. Coexistence curves for $d = 6$, $b_1 = 1$, $b_2 = 0.5$, $q = 0$ black holes. The $p - t$ phase transition diagram displays the novel triple point. The large/small BH transition terminates at the critical point while the small/radiation coexistence line extends up to the maximum pressure.

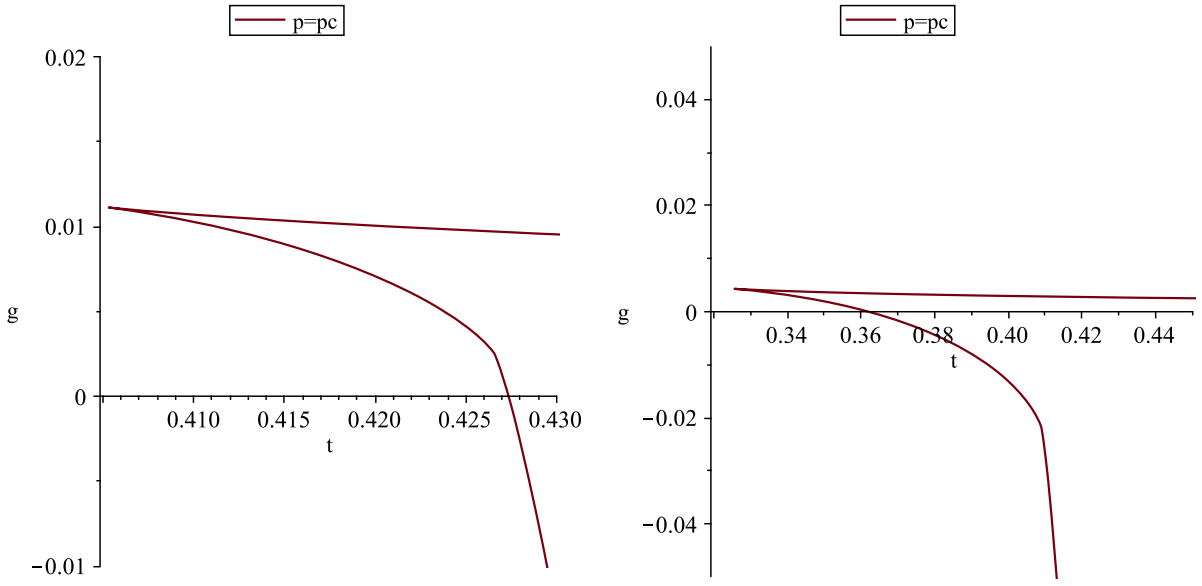

(a) $b_2 = 0.7$ (b) $b_2 = 0.4$

FIG. 12. Comparing the two $g - t$ diagrams with two different values of b_2 and showing the position of the sharp "corner" being above and below the $g = 0$ axis.

consider will possess a vacuum singularity outside the origin.

2. Charged ELBHs

Including charge, the equation of state is now

$$p = \frac{t}{v} - \frac{3b_1}{\pi v^2} + \frac{2tb_1}{v^3} + \frac{q^2}{v^8} - \frac{b_2}{\pi v^4}, \tag{3.54}$$

with Gibbs free energy,

$$g = -\frac{(\frac{1}{4}v^4 + b_1 v^2)(\pi p v^2 + 3b_1 + \frac{b_2}{v^2})}{4\pi v(1 + \frac{2b_1}{v^2})} + \frac{\frac{1}{5}\pi p v^5 + b_1 v^3 + b_2 v}{4\pi} + \frac{q^2(14v^2 + 40b_1)}{96(v^2 + 2b_1)v^3}. \tag{3.55}$$

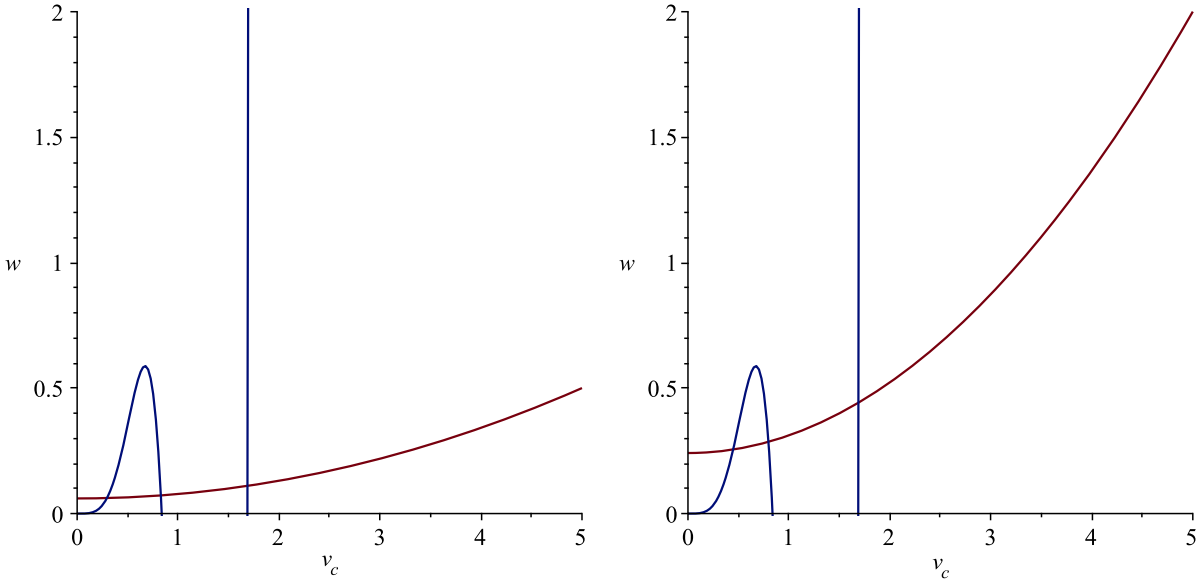

(a) q = 0.01 (b) q = 0.02

FIG. 13. Plots of w_1 (red) and w_2 (blue) in six dimensions for constant charge, showing three intersection between the two functions, giving the possibility of a triple point. Here $b_1 = 0.8$ and $b_2 = 0.5$.

The critical temperature and critical volume relations (3.20) and (3.21) are now

$$t_c = \frac{6b_1 v_c^6 + 4b_2 v_c^4 - 8\pi q^2}{\pi v_c^5 (v_c^2 + 6b_1)} \tag{3.56}$$

$$6v_c^8 b_1 - (36b_1^2 - 12b_2)v_c^6 + 24v_c^4 b_1 b_2 + (-56\pi v_c^2 - 240\pi b_1)q^2 = 0. \tag{3.57}$$

This latter equation is a quartic polynomial in v_c^2; analytic solutions can be obtained, but they are cumbersome, and so we will not display them.

If $b_1 = b_2 = 1$, which corresponds the constant curvature case [8], standard Van der Waals behavior is observed, with a large/small first order transition occurring for $q > 0.1$. This was seen in the five-dimensional case as well, so we shall not display any phase diagrams for this case. Only one critical point is present for $q \geq 0.1$. More interesting behavior occurs for values of $q < 0.1$. We find that more then one critical volume/temperature/pressure is possible, leading to the existence of triple points, previously observed for charged black holes in $d = 6$ Lovelock gravity [8].

To see what happens to the triple point if the horizon curvature is not constant, it is useful to rewrite the critical volume equation (3.57) as

$$w_1 \equiv (56\pi v_c^2 + 240\pi b_1)q^2 = 6v_c^8 b_1 - (36b_1^2 - 12b_2)v_c^6 + 24v_c^4 b_1 b_2 \equiv w_2, \tag{3.58}$$

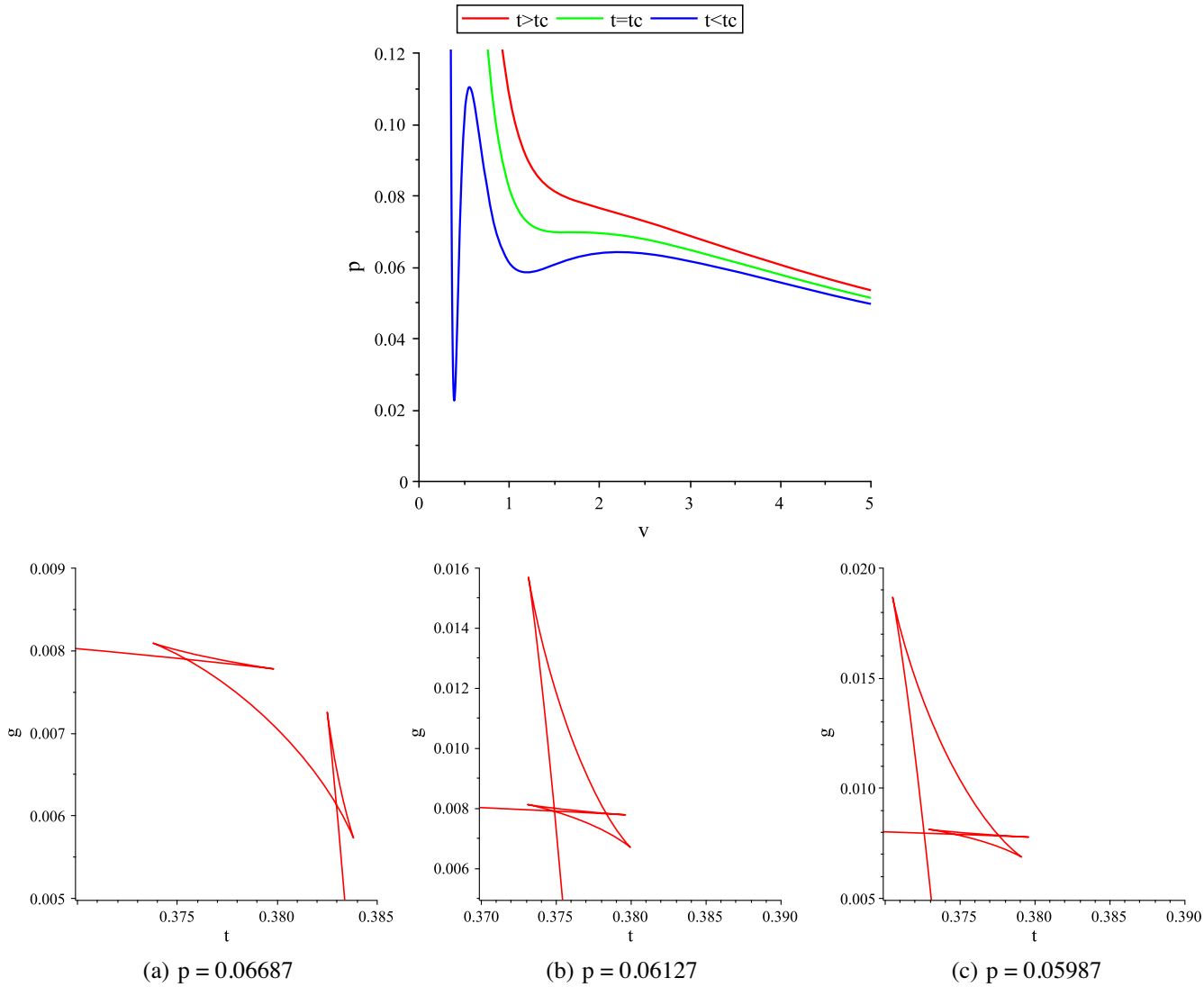

(a) p = 0.06687 (b) p = 0.06127 (c) p = 0.05987

FIG. 14. Phase b for $d = 6$, $q = 0.02$, $b_1 = 0.8$, $b_2 = 0.5$ black holes. Top: The $p - v$ diagram for three constant temperature slices located around the tricritical temperature. We can see in the blue line two oscillations, similar to the constant curvature case. Bottom: Three $g - t$ plots for constant pressure slices are shown. As we decrease the pressure from left to right we see the presence of two swallow tails, which eventually intersect, then separate again.

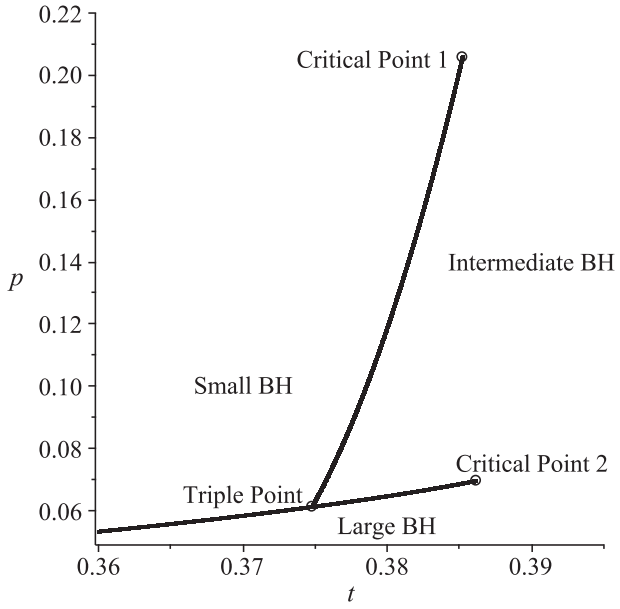

FIG. 15. Coexistence curves for $d = 6$, $b_1 = 0.8$, $b_2 = 0.5$, $q = 0.02$ black holes. We observe the triple point at the intersection of the curves.

and search for the intersection points. A necessary condition for a triple point to occur is that there are three intersection points for $v_c > 0$. This will indeed occur as long as the signs of the coefficients in w_2 alternate—the rule of signs then indicates there are three positive real roots for v_c^2 (and hence for v_c), in turn implying two distinct regions where $w_2 > 0$ for $v_c > 0$, one of which has a maximum. Since w_1 is a quadratic in v_c with coefficient q^2, there will be three intersection points for sufficiently small $q > 0$ and $b_1 > 0$. An example is given in Fig. 13 for $b_1 = 0.8$ and $b_2 = 0.5$. The emergence of the triple point for increasing pressure is shown in Fig. 14, with the phase diagram given in Fig. 15.

We find that for a given value of b_1, the triple point in Fig. 15 moves to the right as b_2 increases. For sufficiently large b_2, the triple point merges with the large/intermediate critical point. Conversely, fixing b_2 and increasing b_1 moves the triple point to the left. This illustrates how changing the horizon geometry of exotic black holes modifies their phase behavior.

IV. SUMMARY AND CONCLUSION

Our investigation of thermodynamic behavior for exotic black holes has uncovered a number of interesting results.

First, concerning the generality of our results, we note that the existence of a formal solution to the field equations for arbitrary values of b_1 and b_2 does not ensure that a base manifold satisfying (2.15) exists for such values. In general the existence of solutions to (2.15) for given (b_1, b_2) is an open question. However it is possible to reverse the roles of our parameters and treat b_1 as a continuous parameter (easily incorporated by adding in a global monopole) while keeping b_2 fixed, which is consistent with the approach considered in [10]. In that case the Bohm $(p, q)_{2m}$ metric was found to be a base manifold satisfying (2.15), and a set of allowed values of b_2 (denoted θ in [10]) were obtained as a function of the integer q. The smallest value $q = 2$ yields $b_2 = 12$. It is straightforward to show that values of $4 < b_1 < 4.24$ exhibit the radiation/large black hole transition, and for $b_1 > 4.24$ the novel triple point occurs. We expect that other base manifolds can likewise be found whose associated black holes display the features we have observed.

Our most interesting result is that of a novel triple point between thermal AdS (radiation), and uncharged large and small black holes in six dimensions. This phase behavior was overlooked in previous studies [8] and arises as a consequence of the exotic geometry of the horizon. We likewise observe a range of large/intermediate/small black hole triple point behavior in the charged case in $d = 6$ as we adjust the parameters of the horizon geometry.

Another interesting result is the generalization (3.8) of massless topological black holes in Einstein gravity [16–18]. For these exotic Gauss-Bonnet black holes two horizons are possible, yielding a richer set of possibilities warranting further study. Negative mass solutions generalizing those in Einstein gravity [16,18] are also possible. We leave a more detailed study of these objects for future investigations.

A study of third order Lovelock gravity, with the possibility of finding a quadruple point, would be interesting. There are two possibilities for a quadruple point. One is that of a novel uncharged quadruple point where we have two swallowtails intersecting each other on the $g = 0$ axis, giving large/intermediate/small/radiation coexistence point. Another would be that in the charged case, where four black holes of distinct size merge at a single point in the phase diagram.

More ambitious endeavours include promoting the topological parameter to a thermodynamic variable itself, generalizations to de Sitter spacetime, and obtaining rotating solutions. Work on these areas is in progress.

ACKNOWLEDGMENTS

This work was supported in part by the Natural Sciences and Engineering Research Council of Canada. We are grateful to Sourya Ray for a number of helpful discussions.

Note added.—Recently, we became aware of a similar study in third order Lovelock gravity [33]. This study considers only uncharged black holes. We do not agree with some of their findings, particularly the failure to notice the presence of Hawking-Page transitions when relevant.

[1] C. M. Will, The confrontation between general relativity and experiment, Living Rev. Relativity **17** (2014).

[2] S. W. Hawking, Particle creation by black holes, Commun. Math. Phys. **43**, 199 (1975).

[3] S. W. Hawking and D. N. Page, Thermodynamics of black holes in anti-de Sitter space, Commun. Math. Phys. **87**, 577 (1983).

[4] D. Kubiznak, R. B. Mann, and M. Teo, Black hole chemistry: Thermodynamics with Lambda, Classical Quantum Gravity **34**, 063001 (2017).

[5] N. D. Birrell and P. C. W. Davies, *Quantum Fields in Curved Space*, Cambridge Monographs on Mathematical Physics (Cambridge University Press, Cambridge, England, 1982).

[6] K. S. Stelle, Renormalization of higher-derivative quantum gravity, Phys. Rev. D **16**, 953 (1977).

[7] D. Lovelock, The Einstein tensor and its generalizations, J. Math. Phys. (N.Y.) **12**, 498 (1971).

[8] A. M. Frassino, D. Kubizňák, R. B. Mann, and F. Simovic, Multiple reentrant phase transitions and triple points in lovelock thermodynamics, J. High Energy Phys. 09 (2014) 80.

[9] S. Ray, Birkhoff's theorem in Lovelock gravity for general base manifolds, Classical Quantum Gravity **32**, 195022 (2015).

[10] G. Dotti and R. J. Gleiser, Obstructions on the horizon geometry from string theory corrections to Einstein gravity, Phys. Lett. B **627**, 174 (2005).

[11] G. Dotti, J. Oliva, and R. Troncoso, Exact solutions for The einstein-Gauss-Bonnet theory in five dimensions: Black holes, wormholes, and spacetime horns, Phys. Rev. D **76** (2007).

[12] G. Dotti, J. Oliva, and R. Troncoso, Vacuum solutions with nontrivial boundaries for the Einstein-Gauss-Bonnet theory, Int. J. Mod. Phys. A **24**, 1690 (2009).

[13] G. Dotti, J. Oliva, and R. Troncoso, Static solutions with nontrivial boundaries for the Einstein-Gauss-Bonnet theory in vacuum, Phys. Rev. D **82** (2010).

[14] J. Oliva, All the solutions of the form $m2(\text{warped}) \times \Sigma(d-2)$ for Lovelock gravity in vacuum in the Chern-Simons case, J. Math. Phys. (N.Y.) **54**, 042501 (2013).

[15] A. Anabalón, F. Canfora, A. Giacomini, and J. Oliva, Black holes with gravitational hair in higher dimensions, Phys. Rev. D **84** (2011).

[16] R. B. Mann, Black holes of negative mass, Classical Quantum Gravity **14**, 2927 (1997).

[17] S. Aminneborg, I. Bengtsson, S. Holst, and P. Peldan, Making anti-de Sitter black holes, Classical Quantum Gravity **13**, 2707 (1996).

[18] W. L. Smith and R. B. Mann, Formation of topological black holes from gravitational collapse, Phys. Rev. D **56**, 4942 (1997).

[19] D. G. Boulware and S. Deser, String-Generated Gravity Models, Phys. Rev. Lett. **55**, 2656 (1985).

[20] R.-G. Cai, A note on thermodynamics of black holes in Lovelock gravity, Phys. Lett. B **582**, 237 (2004).

[21] A. Castro, N. Dehmami, G. Giribet, and D. Kastor, On the universality of inner black hole mechanics and higher curvature gravity, J. High Energy Phys. 07 (2013) 164.

[22] X. O. Camanho and J. D. Edelstein, A Lovelock black hole bestiary, Classical Quantum Gravity **30**, 035009 (2013).

[23] T. Takahashi and J. Soda, Pathologies in Lovelock ads black branes and AdS/CFT, Classical Quantum Gravity **29**, 035008 (2012).

[24] S. Ray, Birkhoff's theorem in Lovelock gravity for general base manifolds, Classical Quantum Gravity **32**, 195022 (2015).

[25] R.-G. Cai, A note on thermodynamics of black holes in Lovelock gravity, Phys. Lett. B **582**, 237 (2004).

[26] A. Castro, N. Dehmami, G. Giribet, and D. Kastor, On the universality of inner black hole mechanics and higher curvature gravity, J. High Energy Phys. 07 (2013) 164.

[27] X. O. Camanho and J. D. Edelstein, A Lovelock black hole bestiary, Classical Quantum Gravity **30**, 035009 (2013).

[28] T. Takahashi and J. Soda, Pathologies in Lovelock AdS black branes and AdS/CFT, Classical Quantum Gravity **29**, 035008 (2012).

[29] T. Jacobson and R. C. Myers, Black Hole Entropy and Higher Curvature Interactions, Phys. Rev. Lett. **70**, 3684 (1993).

[30] D. Kastor, S. Ray, and J. Traschen, Smarr formula and an extended first law for Lovelock gravity, Classical Quantum Gravity **27**, 235014 (2010).

[31] S. Ray, Exotic black holes in Lovelock gravity (2015).

[32] R. B. Mann, Topological black holes: Outside looking in, Ann. Isr. Phys. Soc. **13**, 311 (1997).

[33] N. Farhangkhah and Z. Dayyani, Extended phase space thermodynamics for Lovelock black holes with non-maximally symmetric horizons, Phys. Rev. D **104**, 024068(2021).